

High-Temperature Electrical Conductivity and Electro-mechanical Properties of Stoichiometric Lithium Niobate

G. Ohlendorf, D. Richter, J. Sauerwald, H. Fritze

LaserApplicationCenter, Department of Natural and Materials Sciences,
Clausthal University of Technology, Germany

*Presented on the Bunsen Colloquium: Diffusion and Reactions in Advanced Materials
September 27th – 28th, 2007, Clausthal-Zellerfeld, Germany*

Keywords: stoichiometric LiNbO₃, high-temperature, electrical conductivity, electromechanical properties, oxygen partial pressure dependence

Abstract. High temperature properties such as electrical conductivity (σ) and resonance behaviour of stoichiometric lithium niobate (LiNbO₃) are determined in the temperature range from 20 to 950 °C. The activation energy of the conductivity is found to be 0.9 and 1.7 eV in the temperature range from 500 to 750 °C and from 800 to 950 °C, respectively. During thermal treatments in ambient air up to 950 °C and back, the conductivity remains unchanged at a given temperature, *i.e.*, the crystal is stable under these conditions. The oxygen partial pressure (p_{O_2}) dependence of the conductivity shows two distinct ranges. At 750 °C, the property remains unchanged down to 10^{-15} bar. Below 10^{-15} bar, the conductivity increases according to $\sigma \sim (p_{O_2})^{-1/5}$. Z-cut LiNbO₃ plates can be excited to thickness mode vibrations up to at least 900 °C. At this temperature, the quality factor Q is found to be between 30 and 100. As for changes of the conductivity, a decrease of the resonance frequency is observed below 10^{-15} bar indicating a correlation of both properties. In order to evaluate the lithium evaporation, the crystals are tempered at 900 °C in ambient air for 24 h. A depth profile of the constituents does not indicate lithium loss within the accuracy of the secondary ion mass spectroscopy. The preliminary results underline the potential of stoichiometric LiNbO₃ for high-temperature applications and justify its closer investigation.

1 Introduction

Materials for piezoelectric applications at high temperatures are, *e.g.*, langasite (La₃Ga₅SiO₁₄) and gallium orthophosphate (GaPO₄). In contrast, common piezoelectric materials are not suited for high temperature applications. Quartz shows a phase transformation at 573 °C and high losses above about 400 °C. Long-term stability of non-stoichiometric lithium niobate (Li_{1-x}NbO₃) is observed up to 300 °C, only. Due to decomposition its lifetime is restricted to 10 and 0.1 days at 400 and 450 °C, respectively [1,2,3]. In contrast, stoichiometric LiNbO₃ exhibits potentially attractive optical and piezoelectric properties at elevated temperatures. The phase diagram in [4] shows, that stoichiometric LiNbO₃ has no phase transition up to about 1100 °C. In this paper, electrical and electromechanical properties of stoichiometric

LiNbO₃, in particular the conductivity σ , the resonance frequency f and the resonator quality factor Q , are presented in a temperature range from 20 to 950 °C. The results of the experiments and open questions are discussed.

2 Material and Experimental Methods

2.1 Material

This work is focussed on single crystalline stoichiometric LiNbO₃ manufactured by Crystal Technologies Inc., Palo Alto, USA. The crystals are produced by the Czochralski method. The stoichiometric composition is achieved by subsequent vapour transport equilibration (VTE) of Li_{1-x}NbO₃ wafers. A detailed description of this process is presented in ref. [4]. Such stoichiometric LiNbO₃ is commercially available since recently, only.

The thickness of the Z-cut wafer is 1.35 mm. Samples of 10 × 10 mm² are partially electroded with platinum on both sides. According to this orientation, the piezoelectric excitation results primary in thickness mode vibrations.

2.2 Experimental methods and data evaluation

The resonance behaviour of the crystals is investigated by monitoring the impedance Z in the vicinity of the resonance frequency using a network analyser (HP5100). The fundamental resonance frequency and the overtones are found in a frequency range from 2 to 12 MHz. A specially developed software enables to track the resonance frequency automatically. The impedance data from the resonance spectra are converted into the admittance $Y = Z^{-1}$. The resonator quality factor is given by $Q = (2\pi \times \text{stored energy}) / \text{dissipated energy}$, and obtained from the band width at half maximum of the real part Y' of the admittance squared. In this paper the inverse Q factor is used in order to present a property which is directly proportional to losses.

The conductivity is determined using an impedance analyser (Solartron SI 1260) in the frequency range from 1 Hz to 1 MHz. The low frequency intercept of the RC semicircle in the complex impedance plane is interpreted as bulk resistivity R . By considering the area and the thickness of the sample the conductivity σ is calculated.

Conductivity and resonance frequency measurements are performed in a temperature range from 20 to 950 °C and at oxygen partial pressures (p_{O_2}) from 10⁻³ to 10⁻²⁵ bar. The adjustment of the p_{O_2} is realized using a H₂/H₂O buffer in Ar as carrier gas. Since the evaporation of lithium might be a crucial issue at high temperatures, the lithium content in the vicinity of the surface is determined by Secondary Ion Mass Spectroscopy (SIMS) after annealing the samples in air.

3 Results and Discussion

3.1 Temperature dependence of the conductivity

During thermal treatments in ambient air up to 950 °C and back the conductivity remains unchanged at a given temperature, *i.e.*, the crystals are stable under these conditions. The temperature dependence of the conductivity σ in ambient air is shown in Fig. 1. The Arrhenius plot shows two linear regions which indicate the dominance of two different thermally activated processes. The activation energy E_A is extracted from $\sigma(T) = \sigma_0 \times \exp(-E_A/kT)$ and found to be 0.9 and 1.7 eV in the temperature ranges from 500 to 750 °C (low temperature range) and from 800 to 950 °C (high temperature range), respectively.

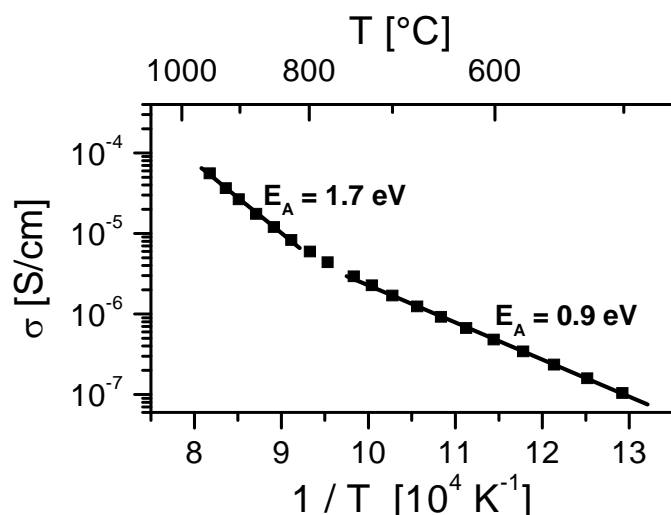


Fig. 1: Temperature dependence of the conductivity from 500 to 950 °C measured in ambient air.

In case of non-stoichiometric LiNbO₃ the transport of lithium is generally suspected to be dominating. On the one hand, the activation energy found for stoichiometric LiNbO₃ in the low temperature range and the values presented in refs. [5,6] (see also Tab. 1) point to predominant lithium transport. On the other hand, in stoichiometric LiNbO₃ the lithium transport might be largely suppressed due to the low concentration of defects. Consequently, the dominance of other species seems to be imaginable. For example, the activation energy for H⁺ in non-stoichiometric Li_{1-x}NbO₃ presented in [7] is in accordance with the result from this work leading to the possibility of dominating hydrogen transport. The presence of hydrogen in form of water vapor cannot be excluded since the conductivity measurements are performed in ambient air.

Tab. 1: Activation energies for the transport of different species (a: recalculated for the conductivity of single crystalline LiNbO₃, b: recalculated for the conductivity of microcrystalline LiNbO₃)

Species	E _A [eV]	Temp. [°C]	Ref.
H (D)	0.87	550 – 650	[7]
Li	1.17	363 – 740	[5]
Li	1.05 ^a	200 – 240	[6]
Li	0.83 ^b	300 – 400	[6]
Li	2.63	820 – 1140	[7]
O	1.43	950 – 1050	[8]
O	3.4	700 – 900	[9]

In the high temperature range a similar discussion applies. Again, the transport of lithium is expected to be dominating for non-stoichiometric LiNbO₃ while other species cannot be excluded for stoichiometric LiNbO₃. For example, the activation energy for the oxygen transport according to ref. [8] agrees roughly with that of the conductivity of stoichiometric LiNbO₃ in the temperature range from 800 to 950 °C. The latter fact points to the possibility of dominating oxygen transport. Significantly higher activation energies for the oxygen transport

in non-stoichiometric LiNbO₃, as presented in ref. [9], are attributed to extrinsic effects and do not apply for this discussion.

Final conclusions should not be drawn based on the preliminary data presented here. Considering the results mentioned above, several conductivity mechanisms might take place. Detailed investigations have to be performed.

3.2 Oxygen partial pressure dependent conductivity

The conductivity is determined as function of p_{O_2} in the range from 10^{-3} to 10^{-25} bar at 750 °C (Fig. 2). Simultaneously, the shift of the fundamental resonance frequency is measured.

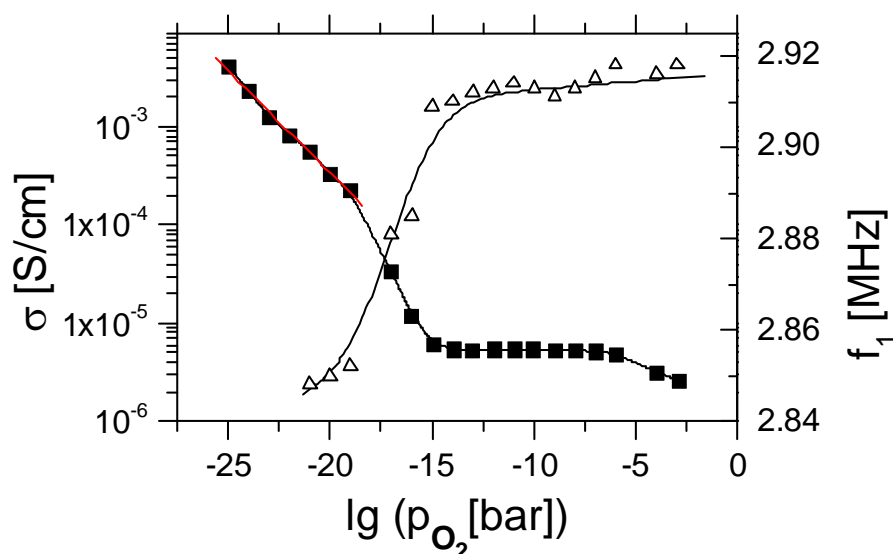


Fig. 2: Conductivity and fundamental resonance frequency as function of the oxygen partial pressure measured at 750 °C.

The conductivity and the resonance frequency are constant down to 10^{-15} bar. Below 10^{-15} bar the conductivity starts to increase. Simultaneously, the resonance frequency decreases. The frequency shift $-\Delta f$ is about 60 kHz in the range from 10^{-15} to 10^{-25} bar which corresponds to 2.1 % of the resonance frequency at high p_{O_2} .

The Sauerbrey equation $\Delta f/f = -\Delta m/m$ or $\Delta f/f = -1/2 \Delta\rho/\rho$ [10] describes the frequency shift of a resonator caused by the deposition of a foreign mass on the surface or by a density change in the material, respectively. Therefore, a decrease in frequency implicates an increase in density which is, however, unlikely with decreasing p_{O_2} . Here, the formation of oxygen vacancies is expected. Therefore we conclude that the mass effect is not responsible for the decrease of the resonance frequency. Changes in the mechanical properties of the resonator material such as mechanical stiffness are potentially the origin of the frequency shift.

Detailed investigations of the defect chemistry of stoichiometric LiNbO₃ must follow and might take advantage of oxygen partial pressure dependence of the conductivity in the range from 10^{-18} to 10^{-25} bar, which is $\sigma \sim (p_{O_2})^{-1/5}$ (see Fig. 2).

3.3 Resonance behaviour at high temperatures

The fundamental frequency and the overtones $f_2 \dots f_4$ are measured in the entire temperature range from 20 to 900 °C. Fig. 3 presents typical resonance spectra at 65 and 900 °C. We found resonance frequencies as listed in Tab. 2 (room temperature values).

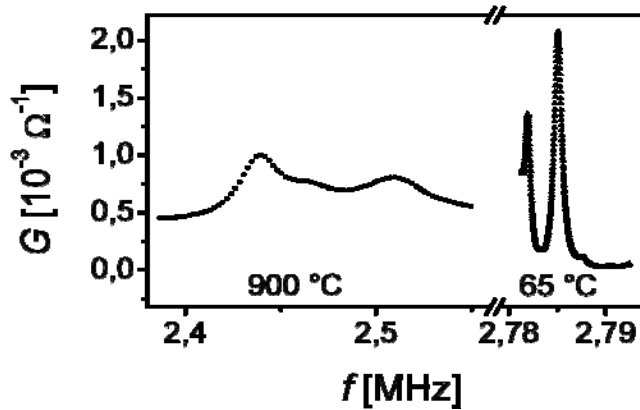


Fig. 3: Typical resonance spectra of the fundamental mode at 65 and 900 °C.

Tab. 2: Resonance frequencies $f_1 - f_4$ at room temperature

	f_1	f_2	f_3	f_4
f [MHz]	2.785	5.458	8.394	10.786

It is remarkable, that stoichiometric LiNbO₃ can be excited to thickness mode vibrations even up to 900 °C. As mentioned above, non-stoichiometric Li_{1-x}NbO₃ shows long-term stability up to 300 °C, only.

Fig. 4 presents the temperature dependence of the resonance frequency f_3 and the associated inverse quality factor Q^{-1} . At low temperatures the frequency decreases with increasing temperature. Above 700 °C the characteristic changes, *i.e.*, the frequency decreases. In con-

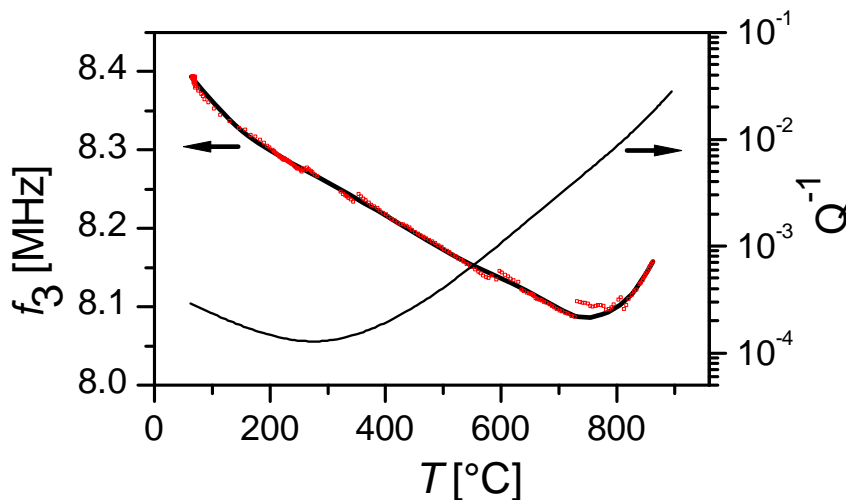


Fig. 4: Temperature dependence of the resonance frequency f_3 and of the inverse quality factor Q^{-1} .

trast, the frequencies f_2 and f_4 decrease with increasing temperature up to 500 °C and increase from 500 to 900 °C. In contrast, the fundamental frequency f_1 is decreasing in the entire temperature range up to 900 °C. Above 400 °C the inverse quality factor Q^{-1} of the frequencies $f_1 \dots f_4$ is monotonously increasing. In this temperature range thermal activated loss mechanisms are expected to be dominating. The maximum of Q is observed below 400 °C and found to be about 10^4 for the resonance modes investigated here.

Fig. 5 shows an Arrhenius plot of the inverse quality factor Q^{-1} of the frequency f_3 in the temperature range from 500 to 900 °C. In order to obtain this plot, a temperature independent

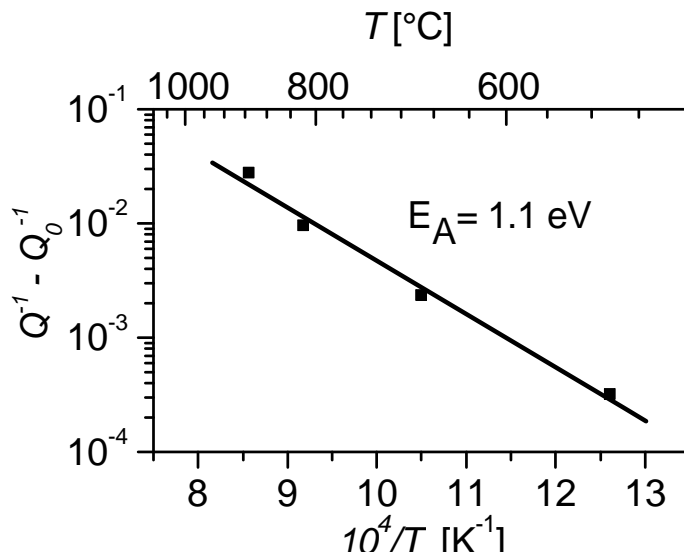


Fig. 5: Arrhenius plot of the inverse quality factor the frequency f_3 from 500 to 900 °C.

contribution Q_0^{-1} is subtracted from Q^{-1} which results in an Arrhenius like behaviour of $Q^{-1} - Q_0^{-1}$. The temperature independent contribution can be interpreted as loss which arises from imperfect resonator design as well as from the electrodes and resonator mounting. In this temperature range the activation energy is about 1.1 eV and corresponds roughly to that of the conductivity in the lower temperature range (see Fig.1).

3.4 Lithium evaporation at high temperatures

In order to evaluate the lithium evaporation, LiNbO₃ crystals are tempered at 900 °C for 24 h in ambient air. A depth profile of the elements Li, Nb and Pt (electrode material) is shown in Fig. 5. Loss of lithium is not observed within the accuracy of this method. This fact is in accordance with the above mentioned reversibility of the conductivity during the temperature treatment up to 950 °C and back.

4 Conclusions

Stoichiometric LiNbO₃ exhibits even at 900 °C remarkable piezoelectric properties. A thermal treatment up to 950 °C and back does not alter the electrical properties. Therefore, the material is a potential candidate for high-temperature piezoelectric applications. Simultaneously, applications might take advantage of the attractive optical properties.

So far, preliminary results are presented. Detailed investigations of the defect chemistry and of the transport mechanisms must be performed to explore the applications limits of stoichiometric LiNbO₃. Further, an advanced understanding is required to tailor the materials properties. Modifications of the materials properties by, *e.g.*, doping are expected to be effec-

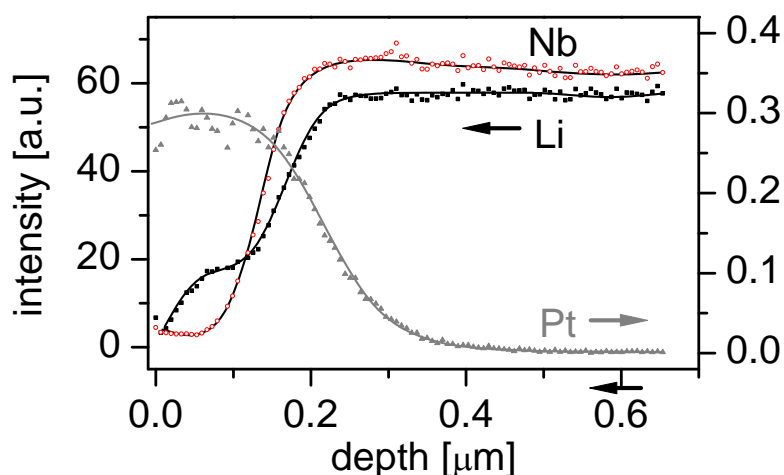


Fig. 5: Depth profile after 24 h annealing at 900 °C in ambient air measured with SIMS.

tive in stoichiometric LiNbO₃ since the largely suppressed lithium non-stoichiometry does not necessarily determine the defect chemistry.

Acknowledgement. The authors thank Dr. D. Jundt, Crystal Technologies Inc., Palo Alto, USA, for providing the stoichiometric LiNbO₃ crystals. Further, we would like to thank Prof. G. Borchardt, Institute of Metallurgy, Clausthal University of Technology, Germany, for the support of the SIMS measurements.

References

- [1] J. Hornsteiner, E. Born, G. Fischerauer, E. Riha, IEEE Int. Freq. Contr. Symp. (1998) 615.
- [2] R. Fachberger, G. Bruckner, G. Knoll, R. Hauser, J. Biniash, L. Reindl, IEEE Trans. Ultrason. Ferroel. Freq. Contr. 51 (2004) 1427.
- [3] G. Bruckner, R. Hauser, A. Stelzer, L. Maurer, L. Reindl, R. Teichmann, J. Biniash, IEEE Int. Freq. Contr. Symp. (2003) 942.
- [4] P. F. Burdai, R. G. Norwood, D. H. Jundt, M. M. Fejer, J. Appl. Phys. 71 (1992) 875.
- [5] N. Schmidt, K. Betzler, M. Grabs, S. Kapphan, F. Klose, J. Appl. Phys. 65 (1989) 1253.
- [6] P. Heitjans, M. Masoud, A. Feldhof, M. Wilkening, Faraday Discussions 134 (2007) 62.
- [7] D. P. Birnie III, J. Mat. Sci. 28 (1993) 302.
- [8] A. Mehta, E. Chang, D. Smyth, J. Mat. Res. 6 (1991) 851.
- [9] P. Fielitz, G. Borchardt, R. De Souza, M. Martin, M. Masoud, P. Heitjans, Solid State Sciences (2008), in press, doi: 10.1016/j.solidstatesciences.2007.11.020
- [10] H. Seh, H. Fritze, H. Tuller, J. Electroceram. 18 (2007) 139.